

# Magnon-Mediated Hall Effect in Kagomé Antiferromagnets

S. A. Owerre<sup>1,2</sup>

<sup>1</sup>*Perimeter Institute for Theoretical Physics, 31 Caroline St. N., Waterloo, Ontario N2L 2Y5, Canada.*

<sup>2</sup>*African Institute for Mathematical Sciences, 6 Melrose Road, Muizenberg, Cape Town 7945, South Africa.*

(Dated: December 9, 2024)

We present a theoretical investigation of topological magnon bands and magnon Hall effect in geometrically frustrated kagomé antiferromagnets with/without Dzyaloshinsky-Moriya interaction (DMI) subject to a magnetic field applied perpendicular to the kagomé plane. For the coplanar/noncollinear  $\mathbf{q} = 0$  spin structure, it is shown that topological magnon bands and the associated magnon Hall effect are absent at zero magnetic field in contrast to previously studied collinear ferromagnets. We show that a finite out-of-plane magnetic field induces a noncoplanar spin texture with nonzero spin scalar chirality and thermal Hall conductivity ( $\kappa_{xy}$ ) is finite even at zero DMI. As the spin scalar chirality is present in the absence of magnetic ordering, these results simply generalize to systems with disordered phases. We propose many experimentally accessible kagomé antiferromagnetic crystals as potential candidates for observing this anomalous effect.

PACS numbers: 66.70.+f, 75.10.Jm

In the classical Hall effect [1] a magnetic field  $\mathbf{B}$  is applied perpendicular to the current  $\mathcal{J}_e$  direction in a metal, as a result the current experiences a Lorentz force  $\mathcal{F} = \mathbf{q} \cdot (\mathbf{v} \times \mathbf{B})$ . The propagation of current is deflected in circular cyclotron orbits by the Lorentz force and charges accumulate on the edge of the material which causes a voltage difference called the Hall voltage. In the quantum case the magnetic orbits are quantized as Landau levels and give rise to a quantized Hall conductivity termed the integer quantum Hall effect [2–4]. Besides, the topology of the electron bands can lead to interesting phenomenon without the influence of the magnetic field. This induces nonzero Berry curvatures and Chern numbers leading to a quantized Hall conductivity termed quantum anomalous Hall effect [5].

The magnetic excitations of ordered quantum magnets are bosonic quasiparticles known as magnons. In these systems the DMI [6] is possible if the magnetic crystal lacks inversion symmetry. The kagomé lattice is built with this property because the midpoints between the bonds connecting the lattice sites are not center of inversion. In collinear ferromagnets, the DMI leads to topological magnon bands even at zero magnetic field [7–16], similar to electronic systems. As magnons are charged-neutral quasiparticles they do not experience the magnetic field in the Lorentz force as in charged particles. Instead, a temperature gradient  $-\nabla T$  transports a heat current  $\mathcal{J}_Q$  and the DMI-induced Berry curvature acts as an effective fictitious magnetic field that deflects the propagation of magnons in the system. The response of the system due to  $-\nabla T$  gives rise to a thermal analog of the Hall effect characterized by a temperature-dependent thermal Hall conductivity tensor  $\kappa_{ij}$  [7, 8]. Thermal Hall effect of magnons and DMI-induced band topology have been studied extensively in single-layer collinear kagomé ferromagnets [7–13, 17, 18]. They were recently observed in an effectively two-dimensional (2D) kagomé ferromagnet Cu(1-3, bdc) [19, 20] and previously reported in 3D pyrochlore ferromagnets [21, 22].

In this Letter, we study a different system with antiferromagnetic interactions. Recently, thermal Hall response has been observed experimentally in frustrated 2D distorted kagomé volborthite  $\text{Cu}_3\text{V}_2\text{O}_7(\text{OH})_2 \cdot 2\text{H}_2\text{O}$  [23]. This is the second kagomé material that shows a finite thermal Hall response. However, in this case a transverse thermal Hall conductivity was observed in a strong magnetic field ( $B_z \sim 15$  Tesla) and no discernible Hall signal was observed at zero field [24]. The observed Hall signal is attributed to spin excitations in the spin liquid (SL) phase. However, a strong field of this magnitude is sufficient to cause magnetic ordering in this crystal [25, 26], although the nature of the ordering and spin Hamiltonian are currently not well-understood. Also in a recent study [27], it has been shown that a strong magnetic field ( $B_z \sim 11$  Tesla) is sufficient to circumvent frustrated interactions and leads to collinear ferromagnetic ordering in frustrated kagomé compound  $\text{Ca}_{10}\text{Cr}_7\text{O}_{28}$ . In other frustrated kagomé materials [28–34], the spins are ordered in  $\mathbf{q} = 0$  patterns at a specific temperature with the spins on each triangle oriented at  $120^\circ$  apart.

In reality, there are more antiferromagnetic systems than ferromagnetic ones, however, the topological magnon bands of kagomé antiferromagnets has received no attention and the mechanism that gives rise to thermal Hall response in frustrated kagomé magnets is not well-understood. In this study, we undertake this task. We carefully scrutinize the noncollinear/coplanar  $\mathbf{q} = 0$  spin structure on the kagomé lattice with DMI, which is known to be the magnetic ordering of most frustrated kagomé magnets [28–34]. However, this system shows trivial magnon bands and we find that  $\kappa_{xy}$  vanishes at zero field in stark contrast to collinear ferromagnets with DMI [7–9, 12, 13, 17–20]. As the out-of-plane magnetic field is turned on, we show that the system exhibits a noncoplanar spin texture with nonzero spin scalar chirality which gives rise to topological magnon bands and nonzero  $\kappa_{xy}$  without the need of DMI. As many frustrated magnets exhibits noncoplanar spin texture with

nonzero spin scalar chirality which survives even in the disordered phase, it is quite possible that this mechanism extends to disordered spin liquid phases of the frustrated kagomé systems. To the best of our knowledge, this is a first study of this model in these contexts. For these reasons, we predict that magnon-mediated thermal Hall response is possible in many frustrated kagomé antiferromagnets in which various compounds with DMI have been synthesized [28–34].

Frustrated kagomé magnetic systems can be synthesized experimentally either in single or bilayer layer forms [27, 29, 30]. Let us begin with bilayer kagomé planes, and assume that the top layer is placed right above the bottom layer forming AAA-stacked pattern. The Hamiltonian is given by

$$\mathcal{H} = \sum_{\langle i,j \rangle \tau} [\mathcal{J} \mathbf{S}_i^\tau \cdot \mathbf{S}_j^\tau + \mathcal{D}_{ij} \cdot \mathbf{S}_i^\tau \times \mathbf{S}_j^\tau] - g\mu_B \mathbf{B} \cdot \sum_{i\tau} \mathbf{S}_i^\tau + \mathcal{J}_t \sum_i \mathbf{S}_i^T \cdot \mathbf{S}_i^B, \quad (1)$$

where  $\mathbf{S}_i$  is the spin moment at site  $i$ ,  $\tau$  labels that top ( $T$ ) and bottom ( $B$ ) layers respectively,  $g$  is the  $g$ -factor and  $\mu_B$  is the Bohr magneton,  $\mathbf{B}$  is an external magnetic field applied perpendicular to the kagomé planes. The inversion symmetry breaking in this system gives rise to a DM vector  $\mathcal{D}_{ij}$ . The last term couples the two layers.

We consider three different cases: (i) layer ferromagnet:  $\mathcal{J}, \mathcal{J}_t < 0$ , (ii) layer antiferromagnet:  $\mathcal{J} < 0, \mathcal{J}_t > 0$ , and (iii) antiferromagnetic insulator on each layer:  $\mathcal{J}, \mathcal{J}_t > 0$ . Case (i) is applicable to the kagomé compound  $\text{Ca}_{10}\text{Cr}_7\text{O}_{28}$ , since a high magnetic field is sufficient to circumvent the frustrated interactions and forces the spins to align in the direction of the external field [27]. It is also applicable to a variant of  $\text{Cu}(1-3, \text{bcd})$  with strong interlayer coupling, since a small out-of-plane field is sufficient to align the spins along the field direction [19, 20]. Case (ii) is applicable to systems in which the spins on the top and bottom layers are oriented in different directions. For these cases the interlayer and intralayer couplings do not introduce spin frustration. However, case (iii) is completely different from the previous ones. It exhibits spin frustration at zero field due to intralayer antiferromagnetic exchange interaction. Nevertheless, it has been pointed out that an out-of-plane DMI [28–36] or an antiferromagnetic second nearest neighbour exchange [37] stabilizes the noncollinear/coplanar  $\mathbf{q} = 0$  spin structure in the single-layer kagomé antiferromagnets. This spin structure also persists for the bilayer system [29]. For this magnetic ordering the interlayer coupling is either ferromagnetic or antiferromagnetic depending on the spin orientations.

We begin with unfrustrated systems, i.e., cases (i) and (ii). We shall start with case (ii) as it recovers case (i) at the saturation field. Classically, the spin operators can be approximated as classical vectors,  $\mathbf{S}_i^\tau = S \mathbf{n}_i^\tau$ , where  $\mathbf{n}_i^\tau = (\sin \chi \cos \theta_i^\tau, \sin \chi \sin \theta_i^\tau, \cos \chi)$  is a unit vector and

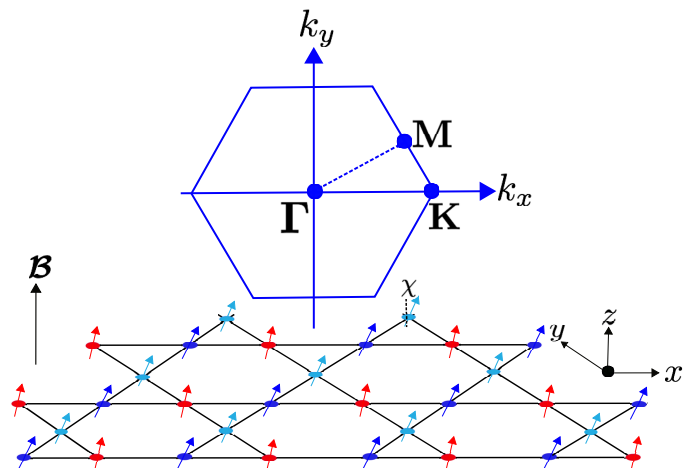


FIG. 1: Color online. Schematics of collinear canted ferromagnet on the bottom layer with coloured arrows denoting different sublattices. For the top layer the spins are rotated by  $180^\circ$ . The magnetic field is applied perpendicular to the plane. The top figure shows the Brillouin zone indicating the high symmetry paths.

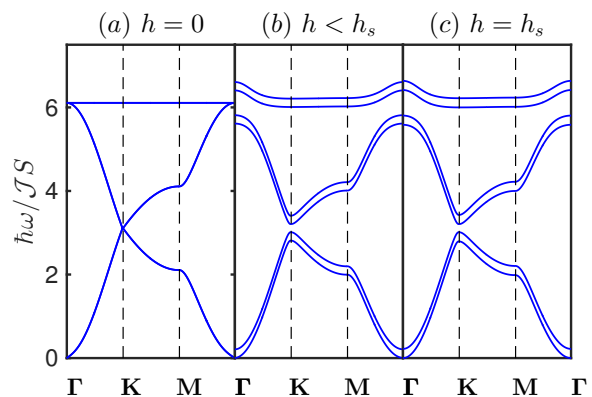


FIG. 2: Color online. Magnon bands of stacked kagomé anti-ferromagnet with  $\mathcal{D} \parallel \mathbf{B}$  at several field values. The parameters are  $\mathcal{D}/\mathcal{J} = 0.12$ ,  $\mathcal{J}_t/\mathcal{J} = 0.11$ .

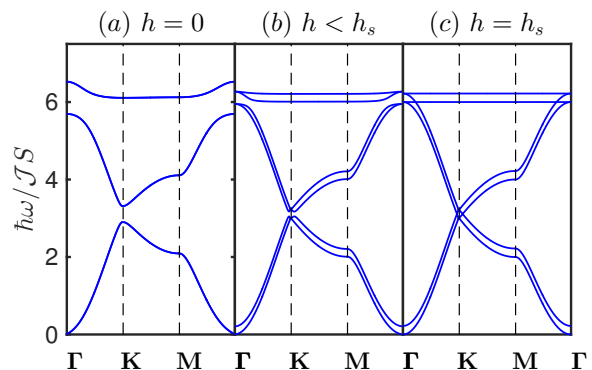


FIG. 3: Color online. Magnon bands of stacked kagomé anti-ferromagnet with  $\mathcal{D} \perp \mathbf{B}$  at several field values. The parameters are  $\mathcal{D}/\mathcal{J} = 0.12$ ,  $\mathcal{J}_t/\mathcal{J} = 0.11$ .

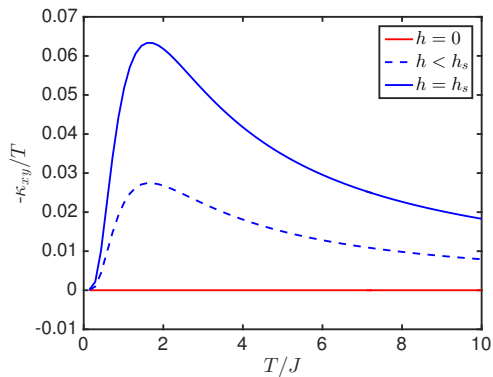


FIG. 4: Color online. Low-temperature dependence of  $\kappa_{xy}$  in stacked spin-1/2 kagomé antiferromagnet for  $\mathcal{D} \parallel \mathcal{B}$  at several field values. The parameters are the same as Fig. 2.

$\theta_i^z$  labels the spin oriented angles on each layer with  $\theta_i^B = 0$  and  $\theta_i^T = \pi$  (see Fig. 1), and  $\chi$  is the field-induced canting angle. The classical energy given by

$$E_{cl}/6NS^2 = -|\mathcal{J}| + \frac{\mathcal{J}_t}{2} \cos 2\chi - h \cos \chi, \quad (2)$$

where  $h = g\mu_B \mathcal{B}_z$  is the out-of-plane field in units of  $S$ , and  $N$  is the number of sites per unit cell. Minimizing the classical energy yields the canting angle  $\cos \chi = h/(h_s = 2\mathcal{J}_t)$ . Notice that both the out-of-plane DMI ( $\mathcal{D} = \mathcal{D}\hat{z}$ ) and the in-plane DMI ( $\mathcal{D} = \mathcal{D}\hat{x}$ ) do not contribute to the classical energy due to ferromagnetic ordering of each layer.

For the excitations above the classical ground state we employ the Holstein-Primakoff spin-boson mapping [38]. The basic procedure is given in Ref. [39]. In this system, both the out-of-plane and the in-plane DMIs contribute to noninteracting magnon model valid at low temperatures. For  $\mathcal{D} \parallel \mathcal{B}$ , the field rescales the out-of-plane DMI as  $\mathcal{D}_z \rightarrow \mathcal{D} \cos \chi$ , whereas for  $\mathcal{D} \perp \mathcal{B}$ , the in-plane DMI is rescaled as  $\mathcal{D}_x \rightarrow \sigma \mathcal{D} \sin \chi$ , where  $\sigma = \mp$  for the bottom and top layers. We have shown the magnon bands of the system in Figs. 2 and 3 along the Brillouin zone paths in Fig. 1, with the parameter values of  $\text{Ca}_{10}\text{Cr}_7\text{O}_{28}$ ,  $\mathcal{J} = 0.76$  meV,  $\mathcal{J}_t = 0.08$  meV [27] and the DM value of  $\text{Cu}(1-3, \text{ bdc})$   $\mathcal{D} = 0.09$  meV [19, 20]. The out-of-plane DM interaction  $\mathcal{D} = \mathcal{D}\hat{z}$  does not contribute at zero field  $h = 0$  ( $\chi = \pi/2$ ) because the spins are along the  $x$ - $y$  kagomé plane and the resulting magnon bands are doubly degenerate between  $S_z \rightarrow S_x = \pm S$  sectors with zero net magnetic moment. There are one flat band and two dispersive bands gapless at the Dirac points  $\mathbf{K} = (\pm 2\pi/3, 0)$ . As the magnetic field increases from zero  $h < h_s$ , each spin has a component along the  $z$ -axis, hence the degeneracy of the bands is lifted and the DM interaction opens a gap at  $\mathbf{K}$ . As the magnetic field approaches the saturation point  $h = h_s$  each layer is fully polarized along the field  $z$ -direction, and the system reduces to layer ferromagnet (case (i)) with gapped magnon bands. For the in-plane DM interaction

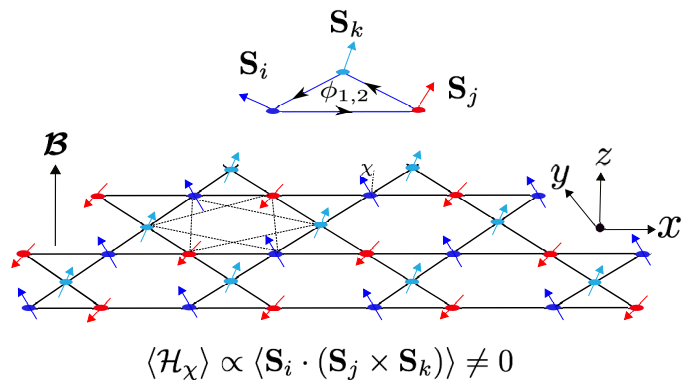


FIG. 5: Color online. Field-induced noncoplanar spin texture on the kagomé antiferromagnet with nonzero spin scalar chirality. The dashed triangle connects the NNN sites and coloured arrows denote different sublattices. The top figure shows the fictitious magnetic fluxes generated by field-induced nonzero spin scalar chirality.

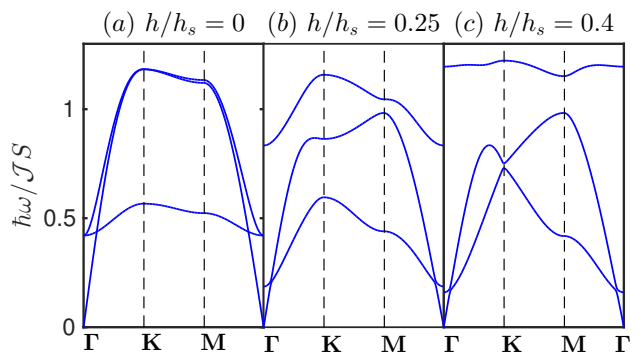


FIG. 6: Color online. Magnon bands of noncollinear  $\mathbf{q} = 0$  single-layer kagomé antiferromagnet with  $\mathcal{D} \parallel \mathcal{B}$  at three field values. The parameters are  $\mathcal{D}_z/\mathcal{J} = 0.06$ ,  $\mathcal{J}_2/\mathcal{J} = 0.03$  and  $\mathcal{J} = 3.34$  meV. This corresponds to the parameter values of  $\text{KFe}_3(\text{OH})_6(\text{SO}_4)_2$  [30].

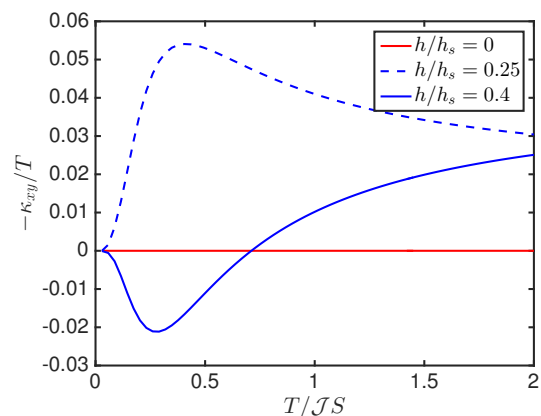


FIG. 7: Color online. Low-temperature dependence of  $\kappa_{xy}$  for  $\text{KFe}_3(\text{OH})_6(\text{SO}_4)_2$  (see Fig. 6) at three field values.

$\mathcal{D} = \mathcal{D}\hat{\mathbf{x}}$ , we have degenerate gapped magnon bands at zero field because the DM contributes since the spins are along the  $x$ - $y$  kagomé plane. As in the previous case, the degeneracy of the bands is lifted at nonzero field and the DM interaction does not contribute at the saturation point  $h = h_s$ , as the spins are fully polarized along the  $z$ -axis, thus, the magnon bands are gapless.

The transverse thermal Hall conductivity  $\kappa_{xy}$  is plotted in Fig. 4 with the formula derived in Ref. [11]. For  $\mathcal{D} \parallel \mathcal{B}$ , the thermal Hall response  $\kappa_{xy}/T$  is negative and vanishes at zero field in accordance with the band structure in Fig. 2(a). In the interval  $h \in (0, h_s)$ , it shows a signal of nonzero values and develops a peak at  $T \sim \mathcal{J}$  before decreasing rapidly towards zero at high temperature. On the other hand, for  $\mathcal{D} \perp \mathcal{B}$  the situation is different. In this case  $\kappa_{xy}$  vanishes in all regimes. This can be understood as follows. At  $h = 0$  the bands are degenerate between  $S_z \rightarrow S_x = \pm S$  sectors with zero net magnetic moment. The Berry curvatures also vanish due to time-reversal symmetry, hence  $\kappa_{xy}$  vanishes similar to anomalous Hall effect in time-reversal-invariant fermionic systems. For  $h < h_s$ , the dispersive bands from the top and bottom layers cross at the  $\mathbf{K}$ -point due to the staggered fluxes of the top and bottom layers [39] and we find vanishing Berry curvatures, again  $\kappa_{xy}$  vanishes. At the saturation field  $h = h_s$ , the DMI does not contribute to noninteracting magnon and the system is gapless, which obviously gives vanishing  $\kappa_{xy}$ .

We are mostly interested in case (iii) as it differs completely from previously studied collinear ferromagnets [7–9, 12, 13, 17–20]. In this case, it suffices to consider single-layer kagomé antiferromagnet  $\mathcal{J}_t = 0$ , applicable to iron jarosite  $\text{KFe}_3(\text{OH})_6(\text{SO}_4)_2$ , an ideal kagomé antiferromagnet with negligible interlayer coupling [29, 30]. The Hamiltonian for this jarosite contains a second-nearest neighbour interaction given by [30]

$$\mathcal{H} = \sum_{i,j} \mathcal{J}_{ij} \mathbf{S}_i \cdot \mathbf{S}_j + \sum_{\langle i,j \rangle} \mathcal{D}_{ij} \cdot \mathbf{S}_i \times \mathbf{S}_j - g\mu_B \mathcal{B}_z \hat{\mathbf{z}} \cdot \sum_i \mathbf{S}_i, \quad (3)$$

where  $\mathcal{J}_{ij} = \mathcal{J}$ ,  $\mathcal{J}_2 > 0$  are the isotropic antiferromagnetic couplings for nearest- (NN) and next-neighbours (NNN) sites respectively. For simplicity, we ignore the in-plane DM component which does not induce any topological magnon bands. Hence, we take  $\mathcal{D}_{ij} = (0, 0, \mp \mathcal{D}_z)$ , where  $-/+$  denotes the directions of the out-of-plane DMI in the up/down triangles as depicted in Fig. 5. They lie in-between the bonds connecting two sites. At zero magnetic field, the out-of-plane DMI [28–34] or  $\mathcal{J}_2 > 0$  [37] stabilizes the coplanar  $120^\circ$  Néel order on the kagomé lattice. However, the magnetic excitations of this noncollinear spin structure do not exhibit nontrivial topological magnon bands even in the presence of DMI [30, 35, 36]. It consists of one nearly flat band (induced by the DMI and a second-nearest neighbour interaction) and two dispersive bands gapless at  $\mathbf{K}$ . Hence, this zero field noncollinear kagomé antiferromagnet is not expected to possess a finite thermal Hall response. To the best of

our knowledge the topological magnon bands of this system has not been studied in any literature. The author has recently been in the forefront of this investigation for the bipartite two-sublattice canted Néel order on the frustrated honeycomb lattice [40].

For the kagomé lattice the situation is completely different as the system is non-bipartite with three-sublattice order, see Ref. [39]. In this case, the magnetic field induces a noncoplanar spin texture with nonzero spin scalar chirality  $\mathcal{H}_\chi \sim \cos \chi \sum \mathbf{S}_i \cdot (\mathbf{S}_j \times \mathbf{S}_k)$ , where  $\cos \chi = h/h_s$  with  $h_s = [6(\mathcal{J} + \mathcal{J}_2) + 2\sqrt{3}\mathcal{D}_z]$ . We see that the scalar chirality changes sign by  $180^\circ$  rotation of the spins, that is  $\mathcal{H}_\chi \rightarrow -\mathcal{H}_\chi$  as  $\chi \rightarrow \pi + \chi$ . It should be noted that the spin scalar chirality can be nonzero even in the absence of magnetic ordering  $\langle \mathbf{S}_j \rangle = 0$ . These observations are one of the main results of this Letter. It is easy to see that  $\mathcal{H}_\chi$  generates fictitious fluxes on the NN and NNN triangular plaquettes of the kagomé lattice as shown in Fig. 5. The magnon bands are shown in Fig. 6 with the parameter values of  $\text{KFe}_3(\text{OH})_6(\text{SO}_4)_2$  [30] which has a negligible interlayer coupling. We see that the bands develop a gap at  $\mathbf{K}$  in the presence of nonzero field. The low-temperature dependence of  $\kappa_{xy}$  is plotted in Fig. 7 with the parameter values of  $\text{KFe}_3(\text{OH})_6(\text{SO}_4)_2$ . We observe that  $\kappa_{xy}$  vanishes at zero field. For nonzero magnetic field, the system is topological [41] with finite thermal Hall conductivity  $\kappa_{xy}$ .

For zero DMI,  $\mathcal{J}_2 > 0$  also stabilizes the  $\mathbf{q} = 0$  coplanar structure [37] as mentioned above. In this case, we also observe a finite  $\kappa_{xy}$  [39] in stark contrast to kagomé ferromagnets [7–9, 12, 13, 19, 20] and frustrated honeycomb lattice [40]. This can be easily understood since for noncoplanar spin structure on non-bipartite lattices, chirality is induced by the field and not the DMI. This is a crucial difference between the present noncollinear/noncoplanar antiferromagnetic model and previously studied collinear ferromagnets on the kagomé lattice [7–9, 12, 13, 19, 20] and two-sublattice canted Néel order on the frustrated honeycomb lattice [40]. It could also explain why thermal Hall response should be finite in the disordered spin liquid phase of frustrated kagomé magnets. Despite the fact that we do not know the nature of magnetic ordering in volborthite at 15 Tesla and the parameter values of the interactions, these results are similar with the trend seen in the kagomé volborthite  $\text{Cu}_3\text{V}_2\text{O}_7(\text{OH})_2 \cdot 2\text{H}_2\text{O}$  [23]. As we have shown, topological effects are absent at zero field in kagomé antiferromagnets [24], as opposed to ferromagnets. Theoretically, the sign change in Fig. 7 is understood as the change in Chern numbers of the system [41]. These results are of particular interest in the ideal kagomé iron jarosite  $\text{KFe}_3(\text{OH})_6(\text{SO}_4)_2$  in which evidence of field-induced spin scalar chirality has been uncovered experimentally [29]. Therefore, there is a high probability of observing finite thermal Hall response in various antiferromagnetic systems with/without DMI [28–34]. This is the main result of this Letter.

In summary, we have shown evidence of finite thermal Hall response in frustrated kagomé antiferromagnets with

noncoplanar spin texture exhibiting nonzero spin scalar chirality induced by the field. An interesting property of our models is that thermal Hall response is absent at zero magnetic field [24], which is not the case in collinear ferromagnets [7–9, 12, 13, 15, 16, 19, 20]. We found that our results show a similar trend recently seen in experiment on the kagomé volborthite  $\text{Cu}_3\text{V}_2\text{O}_7(\text{OH})_2 \cdot 2\text{H}_2\text{O}$  [23] although the nature of the magnetic ordering of this system and the form of the spin Hamiltonian are not well-understood. These results simply generalizes to py-

rochlore antiferromagnets which usually contain kagomé layers along the  $\langle 111 \rangle$  direction. We believe that these results will simulate upcoming experimental kagomé materials with finite thermal Hall response.

The author would like to thank M. Yamashita, for elaborating on the experimental result of thermal Hall response in kagomé volborthite. Research at Perimeter Institute is supported by the Government of Canada through Industry Canada and by the Province of Ontario through the Ministry of Research and Innovation.

- 
- [1] E. H. Hall, *American Journal of Mathematics* **2**, No. 3 (1879), pp. 287-292.
- [2] K. v. Klitzing, G. Dorda, and M. Pepper, *Phys. Rev. Lett.* **45**, 494 (1980)
- [3] R. B. Laughlin, *Phys. Rev. B* **23**, 5632(R) (1981).
- [4] D. J. Thouless, M. Kohmoto, M. P. Nightingale, and M. den Nijs, *Phys. Rev. Lett.* **49**, 405 (1982); M. Kohmoto, *Annals of Physics* **160**, 343 (1985).
- [5] F. D. M. Haldane, *Phys. Rev. Lett.* **61**, 2015 (1988).
- [6] I. Dzyaloshinsky, *J. Phys. Chem. Solids* **4**, 241 (1958); T. Moriya, *Phys. Rev.* **120**, 91 (1960).
- [7] H. Katsura, N. Nagaosa, and P. A. Lee, *Phys. Rev. Lett.* **104**, 066403 (2010).
- [8] R. Matsumoto and S. Murakami, *Phys. Rev. Lett.* **106**, 197202 (2011); *Phys. Rev. B* **84**, 184406 (2011).
- [9] L. Zhang, J. Ren, J. S. Wang, and B. Li, *Phys. Rev. B* **87**, 144101 (2013).
- [10] R. Shindou, R. Matsumoto, S. Murakami, and J. I. Ohe, *Phys. Rev. B* **87**, 174427 (2013).
- [11] R. Matsumoto, R. Shindou, and S. Murakami, *Phys. Rev. B* **89**, 054420 (2014).
- [12] A. Mook, J. Henk, and I. Mertig, *Phys. Rev. B* **90**, 024412 (2014); A. Mook, J. Henk, and I. Mertig, *Phys. Rev. B* **89**, 134409 (2014).
- [13] H. Lee, J. H. Han, and P. A. Lee, *Phys. Rev. B* **91**, 125413 (2015).
- [14] D. Boldrin, B. Fak, M. Enderle, S. Bieri, J. Ollivier, S. Rols, P. Manuel, and A. S. Wills, *Phys. Rev. B* **91**, 220408(R) (2015).
- [15] S. A. Owerre, *J. Phys.: Condens. Matter* **28**, 386001 (2016).
- [16] S. A. Owerre, *J. Appl. Phys.* **120**, 043903 (2016).
- [17] M. Pereiro, D. Yudin, J. Chico, C. Etz, O. Eriksson, and A. Bergman, *Nature Communications* **5**, 4815 (2014).
- [18] A. A. Kovalev and V. Zyuzin, *Phys. Rev. B* **93**, 161106(R) (2016).
- [19] R. Chisnell, J. S. Helton, D. E. Freedman, D. K. Singh, R. I. Bewley, D. G. Nocera, and Y. S. Lee, *Phys. Rev. Lett.* **115**, 147201 (2015).
- [20] Max Hirschberger, Robin Chisnell, Young S. Lee, and N. P. Ong, *Phys. Rev. Lett.* **115**, 106603 (2015).
- [21] Y. Onose, T. Ideue, H. Katsura, Y. Shiomi, N. Nagaosa, Y. Tokura, *Science* **329**, 297 (2010).
- [22] T. Ideue, Y. Onose, H. Katsura, Y. Shiomi, S. Ishiwata, N. Nagaosa, and Y. Tokura, *Phys. Rev. B* **85**, 134411 (2012).
- [23] D. Watanabe, K. Sugii, M. Shimozaawa, Y. Suzuki, T. Yajima, H. Ishikawa, Z. Hiroi, T. Shibauchi, Y. Matsuda, M. Yamashita, *Proc. Natl. Acad. Sci. USA* **113**, 8653 (2016).
- [24] M. Yamashita, Private Communication.
- [25] M. Yoshida, M. Takigawa, H. Yoshida, Y. Okamoto, and Z. Hiroi, *Phys. Rev. Lett.* **103**, 077207 (2009).
- [26] M. Yoshida, M. Takigawa, S. Kramer, S. Mukhopadhyay, M. Horvatic, C. Berthier, H. Yoshida, Y. Okamoto, Z. Hiroi, *J. Phys. Soc. Jpn.* **81**, 024703 (2012).
- [27] C. Balz, B. Lake, J. Reuther, H. Luetkens, R. Schönemann, Th. Herrmannsdörfer, Y. Singh, A. T. M. Nazmul Islam, E. M. Wheeler, J. A. Rodriguez-Rivera, T. Guidi, G. G. Simeoni, C. Baine, and H. Ryll, arXiv:1606.06463; *Nature Physics* (2016).
- [28] M. Elhajal, B. Canals, and C. Lacroix, *Phys. Rev. B* **66**, 014422 (2002).
- [29] D. Grohol, K. Matan, J.H. Cho, S.-H. Lee, J.W. Lynn, D.G. Nocera, Y.S. Lee, *Nature Materials* **4**, 323 (2005).
- [30] K. Matan, D. Grohol, D. G. Nocera, T. Yildirim, A. B. Harris, S. H. Lee, S. E. Nagler, and Y. S. Lee, *Phys. Rev. Lett.* **96**, 247201 (2006).
- [31] O. Cépas, C. M. Fong, P. W. Leung, and C. Lhuillier *Phys. Rev. B* **78**, 140405(R) (2008).
- [32] A. Zorko, S. Nellutla, J. van Tol, L. C. Brunel, F. Bert, F. Duc, J.-C. Trombe, M. A. de Vries, A. Harrison, and P. Mendels, *Phys. Rev. Lett.* **101**, 026405 (2008).
- [33] H. Yoshida, Y. Michiue, E. Takayama-Muromachi, and M. Isobe, *J. Mater. Chem.* **22**, 18793 (2012).
- [34] A. Zorko, F. Bert, A. Ozarowski, J. van Tol, D. Boldrin, A. S. Wills, and P. Mendels, *Phys. Rev. B* **88**, 144419 (2013).
- [35] T. Yildirim and A. B. Harris, *Phys. Rev. B* **73**, 214446 (2006).
- [36] A. L. Chernyshev, *Phys. Rev. B* **92**, 094409 (2015).
- [37] A. B. Harris, C. Kallin, and A. J. Berlinsky, *Phys. Rev. B* **45**, 2899 (1992).
- [38] T. Holstein and H. Primakoff, *Phys. Rev.* **58**, 1098 (1940).
- [39] See Supplemental material.
- [40] S. A. Owerre, arXiv:1608.00545 (2016).
- [41] The topological edge states and Chern numbers of these systems will be studied elsewhere.

# Magnon-Mediated Hall Effect in Kagomé Antiferromagnets Supplemental Material

S. A. Owerre<sup>1,2</sup>

<sup>1</sup>Perimeter Institute for Theoretical Physics, 31 Caroline St. N., Waterloo, Ontario N2L 2Y5, Canada.

<sup>2</sup>African Institute for Mathematical Sciences, 6 Melrose Road, Muizenberg, Cape Town 7945, South Africa.

(Dated: December 9, 2024)

## I. BILAYER KAGOMÉ ANTIFERROMAGNETS

For the excitations above the classical ground state, the general procedure is as follows. At zero field, the spins on each layer lie on the plane of the kagomé lattice taken as the  $x$ - $y$  plane. Then, we perform a rotation about the  $z$ -axis on the sublattices by the spin oriented angles  $\theta_i^\tau$  in order to achieve the layer Néel order, where  $\tau$  labels the top (T) and bottom (B) layers. As the out-of-plane magnetic field is turned on, the spins cant towards the direction of the field. Thus, we have to align them along the new quantization axis by performing a rotation about the  $y$ -axis by the field canting angle  $\chi$ . The rotation matrix is given by

$$\mathcal{R}_z(\theta_i^\tau) \cdot \mathcal{R}_y(\chi) = \begin{pmatrix} \cos \theta_i^\tau \cos \chi & -\sin \theta_i^\tau & \cos \theta_i^\tau \sin \chi \\ \sin \theta_i^\tau \cos \chi & \cos \theta_i^\tau & \sin \theta_i^\tau \sin \chi \\ -\sin \chi & 0 & \cos \chi \end{pmatrix}, \quad (1)$$

with  $\theta_i^B = 0$  and  $\theta_i^T = \pi$ . Hence,

$$\mathbf{S}_i = \mathcal{R}_z(\theta_i) \cdot \mathcal{R}_y(\chi) \cdot \mathbf{S}'_i. \quad (2)$$

Explicitly, Eq. 2 takes the form

$$\begin{aligned} S_{i\tau}^x &= \pm S_{i\tau}'^x \cos \chi \pm S_{i\tau}'^z \sin \chi, \\ S_{i\tau}^y &= \pm S_{i\tau}'^y, \\ S_{i\tau}^z &= -S_{i\tau}'^x \sin \chi + S_{i\tau}'^z \cos \chi, \end{aligned} \quad (3)$$

where  $-(+)$  applies to the  $T(B)$  layers respectively. This rotation does not affect the ferromagnetic  $\mathcal{J}$ -term on each layer. The spin wave [1] Hamiltonian maps to noninteracting magnon tight binding model given by

$$\begin{aligned} \mathcal{H}_{SW} &= v_0 \sum_{i\tau} n_{i\tau} - v_D \sum_{\langle ij \rangle \tau} \left( e^{-i\phi_{ij}} b_{i\tau}^\dagger b_{j\tau} + h.c. \right) \\ &- v_t \sum_{i \in \tau, j \in \tau'} \left[ (n_{i\tau} + n_{j\tau'}) \cos 2\chi + (b_{i\tau}^\dagger b_{j\tau'} + h.c.) \cos^2 \chi \right. \\ &\left. - (b_{i\tau}^\dagger b_{j\tau'}^\dagger + h.c.) \sin^2 \chi \right], \end{aligned} \quad (4)$$

where  $n_{i\tau} = b_{i\tau}^\dagger b_{i\tau}$  is the occupation number,  $v_0 = 4v_J + h \cos \chi$ ,  $v_t = \mathcal{J}_t S$ ,  $v_J = |\mathcal{J}|S$ , and  $v_D = S \sqrt{\mathcal{J}^2 + \mathcal{D}_{x,z}^2}$  with  $\mathcal{D}_z = \mathcal{D} \cos \chi$ ,  $\mathcal{D}_x = \sigma \mathcal{D} \sin \chi$ . The fictitious magnetic flux on each triangle of the Kagomé lattice is given by  $\phi = \arctan(\mathcal{D}_{x,z}/|\mathcal{J}|)$ . Using the vectors  $\Psi_{\mathbf{k}}^\dagger =$

$(\psi_{\mathbf{k}}^\dagger, \psi_{-\mathbf{k}})$ , with  $\psi_{\mathbf{k}}^\dagger = (b_{\mathbf{k}A}^\dagger, b_{\mathbf{k}B}^\dagger, b_{\mathbf{k}C}^\dagger, b_{\mathbf{k}A'}^\dagger, b_{\mathbf{k}B'}^\dagger, b_{\mathbf{k}C'}^\dagger)$ , the momentum space Hamiltonian is given by  $\mathcal{H}_{SW} = \frac{1}{2} \sum_{\mathbf{k}} \Psi_{\mathbf{k}}^\dagger \cdot \mathcal{H}_{AFM}(\mathbf{k}) \cdot \Psi_{\mathbf{k}}$ , where

$$\mathcal{H}_{AFM}(\mathbf{k}) = \begin{pmatrix} \mathbf{A}(\mathbf{k}, \phi) & \mathbf{B} \\ \mathbf{B} & \mathbf{A}^*(-\mathbf{k}, \phi) \end{pmatrix}, \quad (5)$$

$$\mathbf{A}(\mathbf{k}, \phi) = \begin{pmatrix} \mathbf{a}(\mathbf{k}, \phi) & \mathbf{b} \\ \mathbf{b} & \mathbf{a}(\mathbf{k}, \phi) \end{pmatrix}, \quad \mathbf{B} = \begin{pmatrix} 0 & \mathbf{c} \\ \mathbf{c} & 0 \end{pmatrix}, \quad (6)$$

and  $\mathbf{a}(\mathbf{k}, \phi) = \tilde{v}_0 \mathbf{I}_{3 \times 3} - 2v_D \mathbf{\Lambda}(\mathbf{k}, \phi)$ ,

$$\mathbf{\Lambda}(\mathbf{k}, \phi) = \begin{pmatrix} 0 & \cos k_1 e^{-i\phi} & \cos k_3 e^{i\phi} \\ \cos k_1 e^{i\phi} & 0 & \cos k_2 e^{-i\phi} \\ \cos k_3 e^{-i\phi} & \cos k_2 e^{i\phi} & 0 \end{pmatrix}, \quad (7)$$

$$\mathbf{b} = -v_t \cos^2 \chi \mathbf{I}_{3 \times 3}, \quad \mathbf{c} = v_t \sin^2 \chi \mathbf{I}_{3 \times 3}, \quad (8)$$

where  $\mathbf{I}_{3 \times 3}$  is a  $3 \times 3$  identity matrix,  $\tilde{v}_0 = 4|\mathcal{J}|S + h \sin \chi + v_t \cos 2\chi = 4|\mathcal{J}|S + v_t$ ,  $k_i = \mathbf{k} \cdot \mathbf{e}_i$ ,  $\mathbf{e}_1 = (-1/2, -\sqrt{3}/2)$ ,  $\mathbf{e}_2 = (1, 0)$ ,  $\mathbf{e}_3 = (-1/2, \sqrt{3}/2)$ .

## II. NONCOLLINEAR KAGOMÉ ANTIFERROMAGNET

At zero magnetic field, the transverse thermal Hall conductivity vanishes for fully antiferromagnetic quantum systems with Néel-like magnetic ordering. The presence of a nonzero magnetic field gives rise to a canted ordering with finite thermal Hall conductivity. We have analyzed a similar problem in the frustrated honeycomb lattice [2]. In that case, the system is bipartite and the physics is different. Here, we present the analysis for the kagomé antiferromagnet, a non bipartite lattice with three sublattices. We consider the Hamiltonian

$$\mathcal{H} = \sum_{i,j} \mathcal{J}_{ij} \mathbf{S}_i \cdot \mathbf{S}_j + \sum_{\langle i,j \rangle} \mathcal{D}_{ij} \cdot \mathbf{S}_i \times \mathbf{S}_j - h \hat{z} \cdot \sum_i \mathbf{S}_i, \quad (9)$$

where  $\mathcal{J}_{ij} > 0$  are the isotropic antiferromagnetic couplings for nearest- (NN) and next-neighbours (NNN),  $\mathcal{D}_{ij}$  is the DMI between sites  $i$  and  $j$ , and  $h$  is the magnetic field in units of  $g\mu_B$ . At zero field, the  $\mathbf{q} = 0$  ground state in which the spins are oriented  $120^\circ$  apart is stabilized by the next-nearest-neighbour exchange [3] or the symmetry

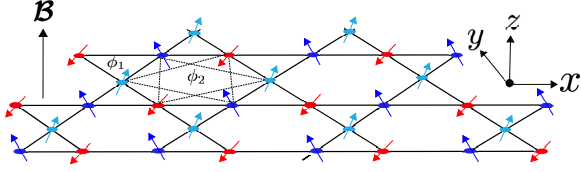


FIG. 1: Color online. Field-induced noncoplanar spin texture on the kagomé antiferromagnet. The dashed triangle connects the NNN sites. The coloured arrows denote different sublattices and  $\phi_{1,2}$  are the field-induced fictitious fluxes on the NN and NNN triangular plaquettes.

breaking out-of-plane DMI,  $\mathcal{D}_{ij} = (0, 0, \mp \mathcal{D}_z)$  [4], where  $-/+$  denotes the directions of the out-of-plane DMI in the up/down triangles as depicted in Fig. 1. The magnon excitations of this ordered state are known both experimentally and theoretically [5, 6]. It consists of one flat band (induced by the DMI) and two dispersive bands which are gapless at  $\mathbf{K} = (\pm 2\pi/3, 0)$  point in the first Brillouin zone. As shown in the main text, such magnon excitations are trivial and do not yield any topological effect, hence thermal Hall conductivity vanishes for such systems.

For nonzero magnetic field, this system has not been studied at least in the topological context. In this case, the noncollinear coplanar  $120^\circ$  Néel order is expected to cant in the direction of the field. To study the excitations of this system, we employ the same rotation as in the bilayer system Eq. 1, where  $\theta_i$  labels the angles in each sublattice with  $\theta_A = 0$  and  $\theta_{B,C} = \pm 2\pi/3$ ,  $\chi$  is the canting angle, and  $\mathcal{D}_{ij} = (0, 0, -\mathcal{D}_z)$  is the out-of-plane DMI. We perform the rotation in Eq. 2. Next, we drop the prime and the corresponding Hamiltonian that contribute to linear spin wave theory is given by

$$\mathcal{H}_{\mathcal{J}} = \mathcal{J} \sum_{\langle i,j \rangle} \left[ \cos \theta_{ij} \mathbf{S}_i \cdot \mathbf{S}_j + \sin \theta_{ij} \cos \chi \hat{\mathbf{z}} \cdot (\mathbf{S}_i \times \mathbf{S}_j) + 2 \sin^2 \left( \frac{\theta_{ij}}{2} \right) [\sin^2 \chi S_{ix} S_{jx} + \cos^2 \chi S_{iz} S_{jz}] \right], \quad (10)$$

$$\mathcal{H}_{\mathcal{J}_2} = \mathcal{J}_2 \sum_{\langle\langle i,j \rangle\rangle} \left[ \cos \theta_{ij} \mathbf{S}_i \cdot \mathbf{S}_j + \sin \theta_{ij} \cos \chi \hat{\mathbf{z}} \cdot (\mathbf{S}_i \times \mathbf{S}_j) + 2 \sin^2 \left( \frac{\theta_{ij}}{2} \right) [\sin^2 \chi S_{ix} S_{jx} + \cos^2 \chi S_{iz} S_{jz}] \right], \quad (11)$$

$$\mathcal{H}_{DMI} = \mathcal{D}_z \sum_{\langle i,j \rangle} \left[ \sin \theta_{ij} [\cos^2 \chi S_{ix} S_{jx} + S_{iy} S_{jy} + \sin^2 \chi S_{iz} S_{jz}] - \cos \theta_{ij} \cos \chi \hat{\mathbf{z}} \cdot (\mathbf{S}_i \times \mathbf{S}_j) \right], \quad (12)$$

$$\mathcal{H}_z = -h \cos \chi \sum_i S_{iz}, \quad (13)$$

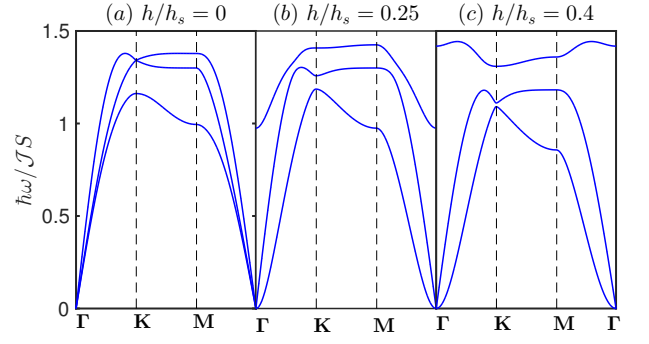


FIG. 2: Color online. Magnon bands of noncollinear  $\mathbf{q} = 0$  kagomé antiferromagnet with zero DMI at three field values. The parameters are  $\mathcal{D}_z/\mathcal{J} = 0.0$ ,  $\mathcal{J}_2/\mathcal{J} = 0.3$ .

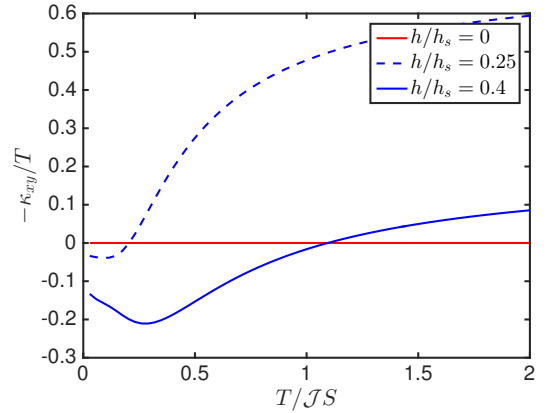


FIG. 3: Color online. Low-temperature dependence of  $\kappa_{xy}$  for the bands in Fig. 2 at three field values.

where  $\theta_{ij} = \theta_i - \theta_j$ . The canting angle is determined from the classical energy

$$E_{cl}/S^2 = \sum_{i,j} \left[ 2(\mathcal{J} + \mathcal{J}_2) \sin^2 \left( \frac{\theta_{ij}}{2} \right) \cos^2 \chi + (\mathcal{J} + \mathcal{J}_2) \cos \theta_{ij} + \mathcal{D}_z \sin^2 \chi \sin \theta_{ij} \right] - h \sum_i \cos \chi, \quad (14)$$

where magnetic field is in units of  $S$ . For the coplanar  $120^\circ$  Néel order, the classical energy is given by

$$E_{cl}/3NS^2 = 2(\mathcal{J} + \mathcal{J}_2) \left( -\frac{1}{2} + \frac{3}{2} \cos^2 \chi \right) - \sqrt{3} \mathcal{D}_z \sin^2 \chi - h \cos \chi. \quad (15)$$

Minimizing this energy yields the canting angle  $\cos \chi = h/h_s$ , with  $h_s = (6(\mathcal{J} + \mathcal{J}_2) + 2\sqrt{3}\mathcal{D}_z)$ . At zero field, we recover the fact that the spins are on the kagomé plane  $\chi = \pi/2$ . The antiferromagnetic system differs from the ferromagnetic system [7–11] in two respects. Firstly,

at zero field  $\chi = \pi/2$  the coefficient of the chiral term  $H_\chi \sim \cos \chi \sum \mathbf{S}_i \cdot (\mathbf{S}_j \times \mathbf{S}_k)$  vanishes and the system is topologically trivial as mentioned above. As we shall show, a nonzero field induces nontrivial bands in the antiferromagnetic system. Secondly, the classical energy depends on the DMI as it contributes to the ground state ordering of the system. This is not the case in ferromagnets. We proceed as usual by introducing the Holstein-Primakoff spin bosonic operators  $S_{ix} = \sqrt{S/2}(b_i^\dagger + b_i)$ ,  $S_{iy} = i\sqrt{S/2}(b_i^\dagger - b_i)$  and  $S_{iz} = S - b_i^\dagger b_i$ , the magnon tight binding Hamiltonian is given by

$$\begin{aligned} \mathcal{H}_2 = S \sum_{i,j} \left[ -\Delta_{ij}^z (b_i^\dagger b_i + b_j^\dagger b_j) + \Delta_{ij} (e^{-i\phi_{ij}} b_i^\dagger b_j + h.c.) \right. \\ \left. + \Delta'_{ij} (b_i^\dagger b_j^\dagger + h.c.) \right] + h_\chi \sum_i b_i^\dagger b_i, \end{aligned} \quad (17)$$

where

$$\Delta_{ij}^z = (\mathcal{J} + \mathcal{J}_2) (\cos \theta_{ij} + 2 \cos^2 \chi \sin^2(\theta_{ij}/2)) + \mathcal{D}_z \sin^2 \chi \sin \theta_{ij} \quad (18)$$

$$\Delta_{1,ij} = \sqrt{(\Delta_{1,ij}^R)^2 + (\Delta_{1,ij}^M)^2}, \quad (19)$$

$$\Delta_{2,ij} = \sqrt{(\Delta_{2,ij}^R)^2 + (\Delta_{2,ij}^M)^2} \quad (20)$$

$$\begin{aligned} \Delta_{1,ij}^R = \mathcal{J} \left[ \cos \theta_{ij} + \frac{2 \sin^2 \chi \sin^2(\theta_{ij}/2)}{2} \right] \\ + \mathcal{D}_z \sin \theta_{ij} \left( 1 - \frac{\sin^2 \chi}{2} \right), \end{aligned} \quad (21)$$

$$\Delta_{1,ij}^M = \cos \chi (\mathcal{J} \sin \theta_{ij} - \mathcal{D}_z \cos \theta_{ij}), \quad (22)$$

$$\Delta_{2,ij}^R = \mathcal{J}_2 \left[ \cos \theta_{ij} + \frac{2 \sin^2 \chi \sin^2(\theta_{ij}/2)}{2} \right], \quad (23)$$

$$\Delta_{2,ij}^M = \mathcal{J}_2 \cos \chi \sin \theta_{ij}, \quad (24)$$

$$\Delta'_{1,ij} = \frac{\sin^2 \chi}{2} (2\mathcal{J} \sin^2(\theta_{ij}/2) - \mathcal{D}_z \sin \theta_{ij}) \quad (25)$$

$$\Delta'_{2,ij} = \mathcal{J}_2 \sin^2 \chi \frac{2 \sin^2(\theta_{ij}/2)}{2}, \quad (26)$$

and  $h_\chi = h \cos \chi$ ,  $\tan \phi_{1,ij} = \Delta_{1,ij}^M / \Delta_{1,ij}^R$ ,  $\tan \phi_{2,ij} = \Delta_{2,ij}^M / \Delta_{2,ij}^R$ . The NNN fictitious flux  $\phi_2$  does not depend on the DMI and originates from the chiral term in the  $\mathcal{J}_2$  coupling. Notice that both fluxes do not vanish at zero DMI unlike in ferromagnets. In momentum space we obtain

$$\begin{aligned} \mathcal{H}_2 = S \sum_{\mathbf{k}, \alpha, \beta; 1,2} (C_{\alpha\beta}^0 \delta_{\alpha\beta} + 2C_{\alpha\beta;1,2}) b_{\mathbf{k}\alpha}^\dagger b_{\mathbf{k}\beta} \\ + C'_{\alpha\beta;1,2} (b_{\mathbf{k}\alpha}^\dagger b_{-\mathbf{k}\beta}^\dagger + b_{\mathbf{k}\alpha} b_{-\mathbf{k}\beta}), \end{aligned} \quad (27)$$

where  $\alpha, \beta = A, B, C$  and the coefficients are given by

$$\mathbf{C}_0 = \text{diag}(\zeta_{AA}, \zeta_{BB}, \zeta_{CC}), \quad (28)$$

with  $\zeta_{\alpha\alpha} = 2[(\mathcal{J} + \mathcal{J}_2) + \sqrt{3}\mathcal{D}_z]$ .

$$\mathbf{C}_{1,2} = \Delta_{1,2;\alpha\beta} \begin{pmatrix} 0 & \gamma_{AB}^{1,2} e^{-i\phi_{1,2}} & \gamma_{CA}^{1,2} e^{i\phi_{1,2}} \\ \gamma_{AB}^{*1,2} e^{i\phi_{1,2}} & 0 & \gamma_{BC}^{1,2} e^{-i\phi_{1,2}} \\ \gamma_{CA}^{*1,2} e^{-i\phi_{1,2}} & \gamma_{BC}^{*1,2} e^{i\phi_{1,2}} & 0 \end{pmatrix}; \quad (29)$$

$$\mathbf{C}'_{1,2} = \Delta'_{1,2;\alpha\beta} \begin{pmatrix} 0 & \gamma_{AB}^{1,2;\alpha\beta} & \gamma_{CA}^{1,2} \\ \gamma_{AB}^{*1,2} & 0 & \gamma_{BC}^{1,2} \\ \gamma_{CA}^{*1,2} & \gamma_{BC}^{*1,2} & 0 \end{pmatrix}; \quad (30)$$

where  $\gamma_{AB}^1 = \cos k_1$ ,  $\gamma_{BC}^1 = \cos k_2$ ,  $\gamma_{CA}^1 = \cos k_3$ ;  $\gamma_{AB}^2 = \cos p_1$ ,  $\gamma_{BC}^2 = \cos p_2$ ,  $\gamma_{CA}^2 = \cos p_3$  and  $k_i = \mathbf{k}_i \cdot \mathbf{e}_i$ ,  $p_i = \mathbf{k}_i \cdot \mathbf{e}'_i$ ,  $\mathbf{e}_1 = (-1/2, -\sqrt{3}/2)$ ,  $\mathbf{e}_2 = (1, 0)$ ,  $\mathbf{e}_3 = (-1/2, \sqrt{3}/2)$ ,  $\mathbf{e}'_1 = \mathbf{e}_3 - \mathbf{e}_2$ ,  $\mathbf{e}'_2 = \mathbf{e}_1 - \mathbf{e}_3$ ,  $\mathbf{e}'_3 = \mathbf{e}_2 - \mathbf{e}_1$ . Here,  $\zeta_{\alpha\alpha}$ ,  $\Delta_{1,2;\alpha\beta}$  and  $\Delta'_{1,2;\alpha\beta}$  are all the same for the coplanar 120° Néel order with  $\theta_A = 0$  and  $\theta_{B,C} = \pm 2\pi/3$ . The Hamiltonian can be written in terms of the Nambu operators  $\mathcal{H}_2 = \mathcal{E}_0 + S \sum_{\mathbf{k}} \Psi_{\mathbf{k}}^\dagger \mathcal{H}(\mathbf{k}) \Psi_{\mathbf{k}}$ , where  $\Psi_{\mathbf{k}}^\dagger = (b_{\mathbf{k}A}^\dagger, b_{\mathbf{k}B}^\dagger, b_{\mathbf{k}C}^\dagger, b_{-\mathbf{k}A}, b_{-\mathbf{k}B}, b_{-\mathbf{k}C})$ . The Hamiltonian to be diagonalized is given by

$$\mathcal{H}(\mathbf{k}) = \begin{pmatrix} \mathbf{C}_0/2 + \mathbf{C}_1 + \mathbf{C}_2 & \mathbf{C}'_1 + \mathbf{C}'_2 \\ \mathbf{C}'_1 + \mathbf{C}'_2 & \mathbf{C}_0/2 + \mathbf{C}_1 + \mathbf{C}_2 \end{pmatrix}. \quad (31)$$

### A. Finite thermal Hall conductivity at zero DMI

As mentioned in the text, the DMI does not provide any topological effects for the noncollinear  $\mathbf{q} = 0$  spin configuration on the kagomé lattice. This means that topological effects persist at zero DMI and nonzero out-of-plane magnetic field via an induced spin scalar chirality  $\mathcal{H}_\chi \sim \cos \chi \sum \mathbf{S}_i \cdot (\mathbf{S}_j \times \mathbf{S}_k)$ , where  $\cos \chi = h/h_s$  with  $h_s = 6(\mathcal{J} + \mathcal{J}_2)$ . However, DMI is usually present on the kagomé lattice due to lack of inversion center. In this section, we show that anomalous magnon Hall effect is present at zero DMI in contrast to collinear ferromagnets. Figures 2 and 3 show the magnon bands and the corresponding  $\kappa_{xy}$  respectively for zero DMI.

[1] T. Holstein and H. Primakoff, Phys. Rev. **58**, 1098 (1940).

[2] S. A. Owerre, arXiv:1608.00545 (2016).

- [3] A. B. Harris, C. Kallin, and A. J. Berlinsky, Phys. Rev. B **45**, 2899 (1992).
- [4] M. Elhajal, B. Canals, and C. Lacroix, Phys. Rev. B **66**, 014422 (2002).
- [5] K. Matan, D. Grohol, D. G. Nocera, T. Yildirim, A. B. Harris, S. H. Lee, S. E. Nagler, and Y. S. Lee, Phys. Rev. Lett. **96**, 247201 (2006).
- [6] A. L. Chernyshev, Phys. Rev. B **92**, 094409 (2015).
- [7] H. Katsura, N. Nagaosa, and P. A. Lee, Phys. Rev. Lett. **104**, 066403 (2010).
- [8] R. Matsumoto and S. Murakami, Phys. Rev. Lett. **106**, 197202 (2011); Phys. Rev. B **84**, 184406 (2011).
- [9] L. Zhang, J. Ren, J. S. Wang, and B. Li, Phys. Rev. B **87**, 144101 (2013).
- [10] A. Mook, J. Henk, and I. Mertig, Phys. Rev. B **90**, 024412 (2014); A. Mook, J. Henk, and I. Mertig, Phys. Rev. B **89**, 134409 (2014).
- [11] H. Lee, J. H. Han, and P. A. Lee, Phys. Rev. B. **91**, 125413 (2015).